Distribution and density of the partition function zeros for the diamond-decorated Ising model

Yen-Liang Chou and Ming-Chang Huang

Department of Physics, Chung-Yuan Christian University, Chung-Li 320, Taiwan

(Received 13 January 2003; published 14 May 2003)

Exact renormalization map of temperature between two successive decorated lattices is given, and the distribution of the partition function zeros in the complex temperature plane is obtained for any decoration level. The rule governing the variation of the distribution pattern as the decoration level changes is given. The densities of the zeros for the first two decoration levels are calculated explicitly, and the qualitative features about the densities of higher decoration levels are given by conjecture. The Julia set associated with the renormalization map is contained in the distribution of the zeros in the limit of infinite decoration level, and the formation of the Julia set in the course of increasing the decoration level is given in terms of the variations of the zero density.

I. INTRODUCTION

About one and half decades ago, spin models defined on hierarchical lattices received much attention in the literature [1–9]. In general, to construct a hierarchical lattice we first start with a unit, which may be a bond or a cell, and then proceed a given type of bond or cell decoration iteratively to the infinite limit. Thus, a hierarchical lattice has fractal structure, and the thermodynamic limit for a physical system defined on a hierarchical lattice is well defined. Hierarchical spin models attract researchers' interest mainly due to two reasons. First, these models are exactly solvable in the context of the Migdal-Kadanoff renormalization scheme [10,11]. Second, owing to the inhomogeneity in the coordination number of lattice sites some particular properties revealed from the models may provide insights to inhomogeneous systems such as random magnets, polymers, and percolation clusters [12].

Q-state Potts model defined on a diamond hierarchical lattice is one example. Starting with a bond, a diamond hierarchical lattice is obtained by replacing bonds by diamonds iteratively to the infinite limit. There exists a remarkable richness of phenomena for the model in the absence of external fields. In particular, the limiting set of the partition function zeros in the complex temperature plane, also referred as the Fisher zeros, are essentially the Julia sets associated with the rational map defined by renormalization transformation [6,7], and the Julia set possesses multifractal structure for $Q>0$ [13–15].

The interest about the loci of partition function zeroes has been raised after the classical works of Yang and Lee on regular lattices [16,17]. After the remarkable Lee-Yang circle theorem, Fisher studied partition function zeros in the complex temperature plane and showed that the distribution is a unit circle in the $\sinh(2J/k_BT)$ complex plane for the two-dimensional zero-field Ising model on simple square lattice [18]. Since then, the distributions of Fisher zeros of the Ising model with isotropic or anisotropic couplings on a variety of classic planar lattices have been investigated [19–22]. Recently Lu and Wu completed the Ising picture by calculating the density of zeros for two-dimensional Ising model in zero field as well as in a pure imaginary field $i\pi/2$ on a variety of

classic planar lattices [23]. In principle, by knowing the zeros of the partition function and the corresponding densities, we may deduce all the thermodynamic characteristics of a system. For example, the density of the zeros near the critical point can be used to extract the critical exponents [20,21], and the logarithmic singularity of the specific heat for the two-dimensional zero-field Ising model is the result of the linearly vanishing density of the zeros near the real axis [18,23].

In this paper we study the distributions and the densities of the Fisher zeros of the zero-field Ising model on square lattices with diamond-type bond decorations, referred as diamond-decorated Ising model (DDIM). The lattices used in the model are constructed by starting with a simple square lattice, and then by implementing diamond-type bond decorations to each bond iteratively to any desired degree. For DDIM, there exists a well-defined thermodynamic limit for any finite degree of decorations, and each primary bond becomes a diamond-hierarchical lattice used in the diamond-hierarchical spin model for the limit of infinite decorations. In our previous work, the properties of ferromagnetic phase transitions of DDIM have been investigated extensively for finite as well as infinite decoration levels [24]. Here we concentrate on the distribution and the density of the Fisher zeros.

Similar analyses on the distribution of the Fisher zeros have been carried out for triangular type Ising lattices with cell decorations [25]. These lattices possess the Sierpiński gasket as the inherent structure for a primary triangle in the limit of infinite decoration level. The results indicate that the distribution of zeros for the infinite decorated lattices coincides with those for the model defined on the Sierpiński gasket, and the distribution of zeros appears to be an union of infinite scattered points and a Julia set called the Jordan curve, and the scattered points are bounded by the Jordan curve. Note that the Jordan curve is a quasi-one-dimensional circle with the Hausdorff dimension equal to 1. It is also well known that the limiting set of the distribution of the zeros of the diamond-hierarchical Ising model (DHIM) is a Julia set, which owns a multifractal structure [6,7,13–15]. The Julia set, which is a bounded planar distribution with the Hausdorff dimension greater than one, is quite different from the
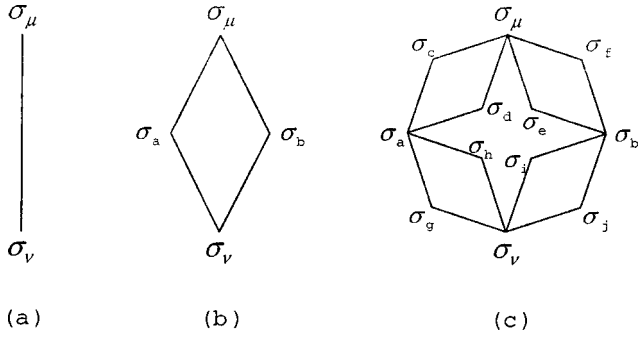
FIG. 1. A decorated bond with the decoration level (a) $n=0$, (b) $n=1$, and (c) $n=2$. Note that the Ising spins with the Latin subscripts are referred as inner spins.

Jordan curve. Based on these observations, we may expect that the Julia set occurring in DHIM may also appear in DDIM, and thence we may understand the formation of the multifractal structure in the Julia set by studying the variation of the distribution and the density of the zeros in the course of increasing the decoration level of DDIM to the infinite limit.

This paper is organized as follows. In Sec. II, we briefly describe how to deduce the exact expression of free energy via the construction of the exact renormalization map of temperature between two successive decoration levels and the use of the known results of the Ising model on simple square lattice. In Sec. III, we study the distribution of the Fisher zeros and exhibit the change of the distribution pattern as the decoration level increases. In Sec. IV, we determine the densities of the zeros for the first two decoration levels by using the results for the case of simple square lattice, and the densities for higher decoration levels are given qualitatively by conjecture. In Sec. V, we discuss how the Julia set arises in the limit of infinite decoration level and characterizes its global mutifractal structure. Finally, Sec. VI is preserved for summary and discussion.

II. FREE ENERGY

We construct the exact expression of the free energy of DDIM with an arbitrary decoration level n in this section. A simple square lattice with diamond-type bond decorations up to the level n is referred as an n lattice. Then, simple square lattice itself is 0-lattice, and its connecting bonds between any two nearest neighbors are named as 0 bonds. We denote the total site number and bond number of 0 lattice as n_s and n_b with $n_b = 2n_s$. A 1 bond is formed by replacing a 0 bond by a diamond that consists of four 0 bonds. Starting with a 0 bond, after the n fold iterative replacements of 0 bonds with 1 bonds, we obtain an n bond that has site number $S^{(n)} = 2(4^n+2)/3$ and 0 bond number $B^{(n)} = 4^n$. An n lattice is formed by replacing all 0 bonds of a 0 lattice with n bonds. For an n lattice, the average site and bond numbers per primary square of 0 lattice are $N_s^{(n)} = 2S^{(n)} - 3$ and $N_b^{(n)} = 2B^{(n)}$, respectively. The construction procedure is schematized in Fig. 1.

The general form of the partition function for DDIM defined on an n lattice reads

$$Z^{(n)} = \sum_{\{\sigma\}} \left[\prod_{\langle i,j \rangle} \exp(\eta \sigma_i \sigma_j) \right], \qquad (1)$$

where the sum is over all bond-connected pairs $\langle i,j \rangle$ of n lattice, and the Ising spin takes two possible values, $\sigma_i = \pm 1$. Here we consider uniform ferromagnetic couplings characterized by the coupling strength J, and the dimensionless coupling parameter η is defined as $\eta = J/k_B T$.

To calculate the partition function of Eq. (1) for an arbitrary n lattice, we use the bond-renormalization scheme in evaluating the Boltzmann factors associated with an n bond. The details of the derivations are given in Ref. [24], and we briefly summarize the results in the followings.

The Boltzmann factor associated with the 0 bond, denoted by $B_{\langle \mu,\nu \rangle}^{(0)}$, is given as $\exp(\eta \sigma_\mu \sigma_\nu)$, and it can be written as

$$B_{\langle \mu,\nu \rangle}^{(0)} = \cosh(\eta) + \sigma_\mu \sigma_\nu \sinh(\eta). \qquad (2)$$

There are decorated $(S^{(n)} - 2)$ sites for an n bond. The Ising spins defined on the decorated sites couple only to those belonging to the same n bond, and we refer them as inner spins. Then we may define the Boltzmann factors associated with an n bond, $B_{\langle \mu,\nu \rangle}^{(n)}$, as the result of taking the sum over the inner spins for the product of all Boltzmann factors associated with the n bond:

$$B_{\langle \mu,\nu \rangle}^{(n)} = \left(\frac{1}{2} \right)^{(S^{(n)} - 2)}$$

$$\times \sum_{\sigma_a, \sigma_b, \ldots, \sigma_s} \exp[\eta(\sigma_\mu \sigma_a + \sigma_a \sigma_b + \cdots + \sigma_s \sigma_\nu)]. \qquad (3)$$

Here the two subscripts μ and ν denote the two primary sites before decorations, the front factor is added for the normalization of the sum, and the sum is over the $(S^{(n)} - 2)$-inner spins. By substituting the expression of Eq. (2) into each Boltzmann factor of Eq. (3), we have

$$B_{\langle \mu,\nu \rangle}^{(n)} = R^{(n)}(\eta)[\cosh(\eta^{(n)}) + \sigma_\mu \sigma_\nu \sinh(\eta^{(n)})], \qquad (4)$$

for $n \geq 1$, where the function $R^{(n)}(\eta)$ is given as

$$R^{(n)}(\eta) = \prod_{k=1}^{n} [\exp(\eta^{(k)})]^{4^{n-k}}, \qquad (5)$$

and $\eta^{(k)}$ is determined by the recursion relation,

$$\exp(\eta^{(k)}) = \cosh(2\eta^{(k-1)}), \qquad (6)$$

with the initial condition $\eta^{(0)} = \eta$ for $1 \leq k \leq n$.

It is well known that the corresponding free energy per bond per $k_B T$ of Eq. (1) for the case of 0 lattice can be written as

$$f^{(0)} = -\frac{1}{4} \ln \sinh(2\eta) - \frac{1}{4} \int_0^{2\pi} \frac{d\phi}{2\pi} \int_0^{2\pi} \frac{d\theta}{2\pi}$$

$$\times \ln \left[\sinh(2\eta) + \frac{1}{\sinh(2\eta)} - \Theta(\theta,\phi) \right], \qquad (7)$$

with

$$\Theta(\theta,\phi)=\cos\theta+\cos\phi. \tag{8}$$

By observing that up to a factor $R^{(n)}(\eta)$ the effective Boltzmann factor of an n bond possesses the same form as that of a 0 bond, we can express the free energy density of an n lattice as [24]

$$f^{(n)}=f_D^{(n)}-\frac{1}{4B^{(n)}}\ln\sinh(2\,\eta^{(n)})-\frac{1}{4B^{(n)}}\int_0^{2\pi}\frac{d\phi}{2\pi}\int_0^{2\pi}\frac{d\theta}{2\pi}$$

$$\times\ln\left[\sinh(2\,\eta^{(n)})+\frac{1}{\sinh(2\,\eta^{(n)})}-\Theta(\theta,\phi)\right], \tag{9}$$

where $f_D^{(n)}$ is the contribution from the factor $R^{(n)}(\eta)$,

$$f_D^{(n)}=-\frac{1}{B^{(n)}}\ln R^{(n)}(\eta), \tag{10}$$

which can be expressed as

$$f_D^{(n)}=-\sum_{k=1}^{n}\frac{1}{4^k}\ln[\cosh(2\,\eta^{(k-1)})], \tag{11}$$

by using the recursion relation of Eq. (6). Note that the $f_D^{(n)}$ part exists only for $n\geqslant1$.

III. FISHER ZEROS

The partition function zeros of a 0 lattice in the thermodynamic limit can be obtained by setting the argument of the logarithm in the free energy density of Eq. (7) equal to zero [23]. It is known that the zeros may lie on the unit circle $|\sinh(2\eta)|=1$ [23] or on two circles $|\tanh(\eta)\pm1|=\sqrt{2}$ [18], depending on the variable used for the complex temperature plane. In this paper, we study the distribution and density of the Fisher zeros in the complex $\tanh(\eta)$ plane. The basic features appearing in the complex $\sinh(2\eta)$ plane are essentially the same as those we obtain in the complex $\tanh(\eta)$ plane.

By observing the free energy density of Eq. (9), in the thermodynamic limit we can obtain the distribution of zeros of an n lattice from the solutions of two conditions,

$$\sinh(2\,\eta^{(n)})+\frac{1}{\sinh(2\,\eta^{(n)})}-\Theta(\theta,\phi)=0 \tag{12}$$

and

$$\cosh(2\,\eta^{(k-1)})=0 \quad \text{for} \ k=1,2,\ldots,n. \tag{13}$$

Note that the latter can also be viewed as the condition of the zeros for the Ising system defined on an n bond, and such a system becomes DHIM in the limit of infinite n.

From the result of two circles for the partition function zeros of a 0 lattice in the complex $\tanh(\eta)$ plane, we may conclude that the solution of Eq. (12) is two circles in the complex $\tanh(\eta^{(n)})$ plane:
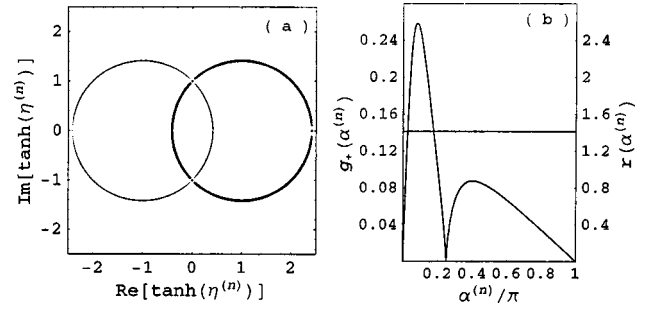

FIG. 2. (a) The distribution of the Fisher zeros of an n lattice in the complex $\tanh(\eta^{(n)})$ plane as the left (gray) and the right (bold-faced) n cycle, and (b) the density (left vertical scale) and the radius (right vertical scale) of the Fisher zeros in the left n cycle.

$$|\tanh(\eta^{(n)})\pm1|=\sqrt{2}. \tag{14}$$

The two circles intersect at two points, i and $-i$. As shown in Fig. 2(a), due to the intersections there is a ring contained in the two circles. For the purpose of identification, we refer the circles as two n cycles and the ring as n ring. Note that in displaying the distributions of zeros, we always use bold-faced curves for the right n cycle and its descendants, and gray curves are for those from the left n cycle. This distribution also appears to have the symmetry of inversion about the center $\tanh(\eta^{(n)})=0$.

For the purpose of comparing the distributions of zeros among different n lattices, we have to bring the zeros to the complex plane of an unique variable chosen to be $\tanh(\eta)$. To achieve this, we notice that the recursion relation of Eq. (6) can be rewritten as

$$\tanh(\eta^{(n)})=\frac{2[\tanh(\eta^{(n-1)})]^2}{1+[\tanh(\eta^{(n-1)})]^4}, \tag{15}$$

which has the inverse map given as

$$\tanh(\eta^{(n-1)})=\pm\left(\frac{1\pm\sqrt{1-[\tanh(\eta^{(n)})]^2}}{\tanh(\eta^{(n)})}\right)^{1/2}. \tag{16}$$

Then, starting with the two n cycles in the complex $\tanh(\eta^{(n)})$ plane, we can obtain the corresponding distribution of zeros in the complex $\tanh(\eta)$ plane by performing the n fold backward iterations provided by Eq. (16).

After the first backward iteration, we show the resultant distribution in the complex $\tanh(\eta^{(n-1)})$ plane in Fig. 3(a) where the points indicated by crosses are the preimages of the map of Eq. (15) for the centers of two n cycles, 1 and -1. The results indicate that each of the n cycles shown in Fig. 2(a) splits in to two closed curves referred as $(n-1)$ cycles. There are eight intersection points between the descendants of the right n cycle and those from the left n cycle, and the loci of the intersections are determined by the inverse maps of the points, i and $-i$, which are the intersections of two n cycles. There are four rings, referred as $(n-1)$ rings, caused by the intersections. Note that the distri-
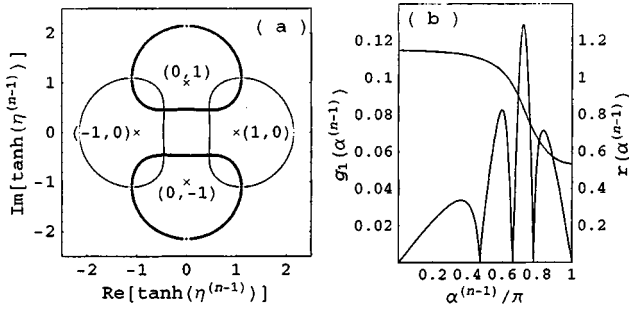
FIG. 3. (a) The four $(n-1)$ cycles for the zero distribution of an n lattice in the complex $\tanh(\eta^{(n-1)})$ plane. The cycles displayed by the bold-faced curves are the descendants of the right n circle and the gray curves are those from the left n circle. The points indicated by crosses are taken as the centers of the $(n-1)$ cycles, and they are the preimages of the renormalization map for the centers of two n cycles. (b) The density (left vertical scale) and the radius (right vertical scale) of the Fisher zeros in the $(n-1)$ cycle with the center at $(1,0)$.

bution shown in Fig. 3(a) are just the distribution of zeros in the complex $\tanh(\eta)$ plane subject to the condition of Eq. (12) for an 1 lattice.

Proceeding with the inverse map given by Eq. (16) from the complex variable $\tanh(\eta^{(n-1)})$ to $\tanh(\eta^{(n-2)})$ for the four $(n-1)$-cycles, we obtain 12 $(n-2)$ cycles, as shown in Fig. 4(a). The $(n-2)$ cycles contain 16 $(n-2)$ rings caused by the 32 intersections among the cycles. The intersections are again the preimages of the map of Eq. (15) for the loci of the intersections among the $(n-1)$ cycles.

Continuing with this procedure, we show the distribution of zeros in Fig. 5 for $n=4$ and Fig. 6 for $n=8$. In general, the zero distribution for a n lattice in the complex $\tanh \eta$ plane, subject to the condition of Eq. (12), is the union of $[2+2(4^{n}-1)/3]$ 0 cycles, which have $4^{n+1}/2$ intersections, and these intersections yield 4^{n} 0 rings contained in the 0 cycles. The 0 cycles can be divided into two classes: one consists of the descendants of the left n cycle with $[2+2(4^{n-1}-1)/3]$ members and the other has $4^{n}/2$ members, which are the descendants of the right n cycle. The intersections only occur between two 0 cycles belonging to different class. The distribution always maintain the inversion symmetry about the center $\tanh \eta = 0$.

For the condition of Eq. (13), it can be rewritten in terms of the $\tanh \eta^{(n)}$ variable as

$$\tanh \eta^{(k-1)} = \pm i \quad \text{for} \quad k=1,2,\ldots,n. \quad (17)$$

Then, for the case of $n=1$ the two zeros, i and $-i$, in the complex $\tanh \eta$ plane are just the intersection points of two n cycles in the complex $\tanh(\eta^{(1)})$ plane. Proceeding to the case of $n=2$, we obtain, besides of the previous two zeros, eight more points in the complex $\tanh(\eta)$ plane from $k=2$ in Eq. (17). These additional points are the preimages of the renormalization map for the original two points, and they are the intersection points among four $(n-1)$ cycles in the complex $\tanh(\eta^{(n-1)})$ plane. By induction, we may conclude that the zeros in the complex $\tanh(\eta)$ plane obtained from condition of Eq. (17) are $2(4^{n}-1)/3$ scattered points which
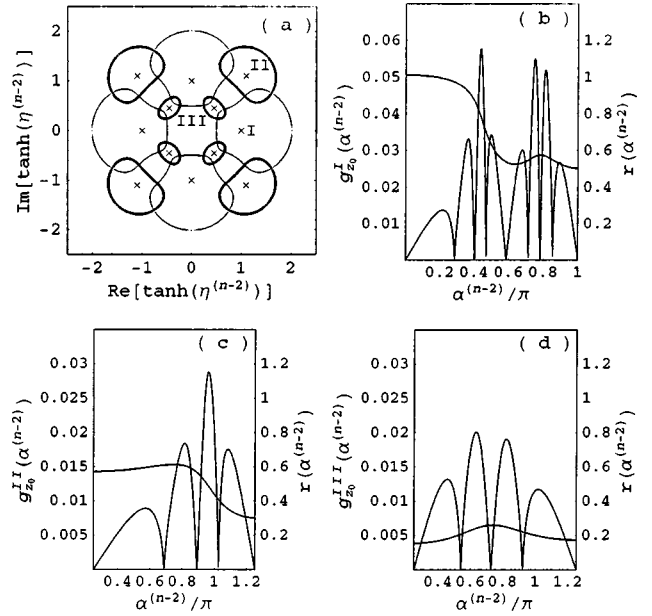

FIG. 4. (a) The 12 $(n-2)$ cycles for the zero distribution of an n lattice in the complex $\tanh(\eta^{(n-2)})$ plane. The points indicated by crosses are taken as the centers of the $(n-2)$ cycles, and they are the preimages of the renormalization map for the centers of the $(n-1)$ cycles. The 12 $(n-2)$ cycles can be divided into three classes, I, II, and III, according to the decreasing order in the magnitude of the circumference of a circle. The density (left vertical scale) and the radius (right vertical scale) of (b) the $(n-2)$ cycle, which is the one marked I in (a), with the center coordinate $(1,0)$; (c) the $(n-2)$ cycle, which is the one marked II in (a), with the center coordinate $\sqrt{1+\sqrt{2}}e^{i\pi/4}$; and (d) the $(n-2)$ cycle, which is the one marked III in (a), with the center coordinate $\sqrt{-1+\sqrt{2}}e^{i\pi/4}$.

are the union of the intersection points among k cycles in the complex $\tanh(\eta^{(k)})$ plane for $1 \leq k \leq n$. in the complex $\tanh(\eta)$ plane for an n lattice.

Thus, we can describe the distribution pattern of the Fisher zeros of DDIM with the decoration level n in the complex $\tanh(\eta)$ plane as follows. There are $2(4^{n}-1)/3$ scattered points given by Eq. (17). In addition, there are $[2+2(4^{n}-1)/3]$ 0 cycles with 2×4^{n} intersections obtained from Eq. (12).

Among all the zeros we obtained in the above, as a consequence of the Lee-Yang theorem [16,17], the bulk critical points correspond to the zeros falling on the physical region. The physical region of the variable $\tanh(\eta)$ is $0 \leq \tanh(\eta) < 1$ for ferromagnetic couplings $\eta \geq 0$. This implies that the variable $\tanh(\eta^{(n)})$ also takes the range $0 \leq \tanh(\eta^{(n)}) < 1$ as the physical region for any n value.

From the solutions of the conditions of Eqs. (12) and (13), we know that there is only one zero in the physical region. This zero belongs to the right n cycle and locates at

$$\tanh(\eta^{(n)}) \overset{c}{=} h^{(0)}, \quad (18)$$

with $h^{(0)} = \sqrt{2}-1$ for arbitrary decoration level n. Here, for convenience, we use the notation " $\overset{c}{=}$ " to denote the equality

FIG. 5. The zero distribution of an n lattice in the complex $\tanh(\eta)$ plane obtained from the condition of Eq. (12) for $n=4$.
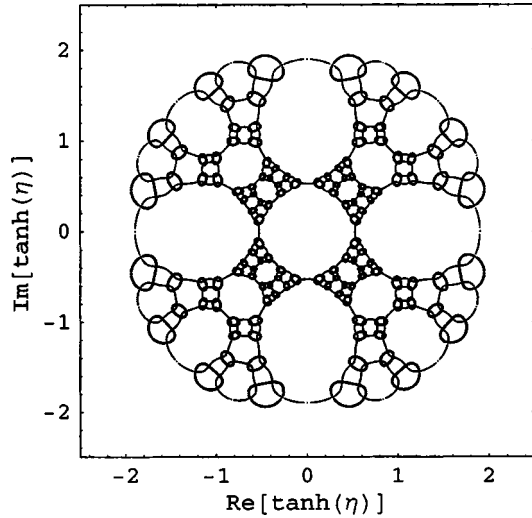

FIG. 6. The zero distribution of an n lattice in the complex $\tanh(\eta)$ plane obtained from the condition of Eq. (12) for $n=8$.

established only at the phase transition point. Note that the $h^{(0)}$ value is just the reduced critical temperature, $\tanh(J/k_B T_c)$, of the ferromagnetic phase transition for the square Ising model, i.e., $n=0$.

To find the locus of the zero specified by Eq. (18) in the complex $\tanh(\eta)$ plane, we can continuously use the inverse map of Eq. (16) to obtain the equivalent expression of Eq. (18) as

$$\tanh(\eta^{(n-k)}) \overset{c}{=} h^{(k)}, \tag{19}$$

with

$$h^{(k)} = \left(\frac{1 - \sqrt{1 - (h^{(k-1)})^2}}{h^{(k-1)}} \right)^{1/2} \tag{20}$$

for $1 \leq k \leq n$. Note that in obtaining Eq. (20) for the critical value of $\tanh(\eta^{(n-k)})$ we have used the constraint $0 \leq \tanh(\eta^{(n-k)}) < 1$.

Thus, the zero $h^{(0)}$ in the complex $\tanh(\eta^{(n)})$ plane corresponds to the zero $h^{(n)}$ in the complex $\tanh(\eta)$ plane, and the $h^{(n)}$ value is just the reduced critical temperature $\tanh(J/k_B T_c)$ of the ferromagnetic phase transition for DDIM with the decoration level n. The sequence of $h^{(n)}$ decreases as n increases, and the $h^{(n)}$ value in the limit of infinite n is given by the asymptotic value of the sequence of $h^{(n)}$. For the recursion relation of Eq. (15), there are three fixed points, one repellor locating at $0.5437\ldots$, and two attractors at 0 and 1. Since the $h^{(n)}$ value is obtained from $h^{(0)}$ via the n fold backward iterations given by Eq. (20) and the attractors (repellors) of the map become the repellors (attractors) of the inverse map, we may conclude that the $h^{(n)}$ value is the locus of the repellor of Eq. (15), $h^{(n)} = 0.5437\ldots$, for the case of infinite n.
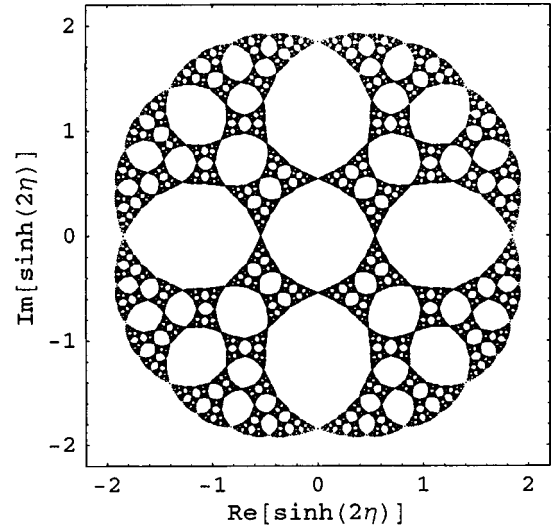
IV. DENSITY OF ZEROS

The density of two n cycles in the complex $\tanh(\eta^{(n)})$ plane has been determined by Lu and Wu [23]. Based on this result, we determine the density of the zeros of DDIM in this section by performing proper transformations. First, we describe the result of Lu and Wu briefly in the following.

The two cycles of Eq. (14) are written as

$$\tanh(\eta^{(n)}) \pm 1 = r(\alpha^{(n)}) \exp(i\alpha^{(n)}), \tag{21}$$

where $r(\alpha^{(n)}) = \sqrt{2}$ is the radial distance from the center coordinate. By considering an $M \times 2N$ simple-quartic lattice with Brascamp-Kunz boundary condition, we introduce the zero density $g_\pm(\alpha^{(n)})$, that satisfies the normalization condition

$$\int_0^{2\pi} g_\pm(\alpha^{(n)}) d\alpha^{(n)} = \frac{1}{2}, \tag{22}$$

such that the number of zeros in the interval $[\alpha^{(n)}, \alpha^{(n)} + d\alpha^{(n)}]$ is $2MN g_\pm(\alpha^{(n)}) d\alpha^{(n)}$ for the left ($+$) and right ($-$) n cycle, respectively. The zero density is given as

$$g_+(\alpha^{(n)}) = g_-(\pi - \alpha^{(n)}) = \left(\frac{x}{\pi^2} \right) \left| \frac{1 - \sqrt{2} \cos \alpha^{(n)}}{3 - 2\sqrt{2} \cos \alpha^{(n)}} \right| K(x), \tag{23}$$

where

$$x = \frac{2|\sin \alpha^{(n)}|(\sqrt{2} - \cos \alpha^{(n)})}{3 - 2\sqrt{2} \cos \alpha^{(n)}}, \tag{24}$$

and $K(x)$ is the complete elliptic integral of the first kind,

$$K(x) = \int_0^{\pi/2} dt \frac{1}{\sqrt{1 - x^2 \sin^2 t}}. \tag{25}$$

The density of $g_+(\alpha^{(n)})$, which has the symmetry $g_+(\alpha^{(n)})=g_+(2\pi-\alpha^{(n)})$, is plotted in Fig. 2(b) for the range $0\leq\alpha^{(n)}\leq\pi$. Here we also specify the radial distance of a zero, $r(\alpha^{(n)})$, in the right vertical scale. For small $\alpha^{(n)}$, the result of Eq. (23) has the linear behavior as

$$g_\pm(\alpha^{(n)})=\left(\frac{3\pm2\sqrt{2}}{\pi}\right)|\alpha^{(n)}|. \quad (26)$$

Note that the density $g_+(\alpha^{(n)})$ of the zeros near the point $\alpha^{(n)}=0$ is the same as the density $g_-(\alpha^{(n)})$ near the point $\alpha^{(n)}=\pi$, which is the ferromagnetic phase transition point of the bulk system, and this linearly vanishing density of the zeros near the bulk transition point leads to the logarithmic singularity of the specific heat.

To find the corresponding density in the complex $\tanh(\eta^{(n-1)})$ plane, we first write the $(n-1)$ cycles as

$$\tanh(\eta^{(n-1)})=z_0+r(\alpha^{(n-1)})\exp(i\alpha^{(n-1)}). \quad (27)$$

Here the center coordinates z_0 are chosen to be the preimages of the map of Eq. (15) for the center coordinates of n cycles, $\tanh(\eta^{(n)})=1$ and -1, and this leads to $z_0=1$, -1, i, and $-i$ for the center coordinates of four $(n-1)$ cycles. The zero density of the $(n-1)$ cycle, specified by the center coordinate z_0, is denoted as $g_{z_0}(\alpha^{(n-1)})$, and we have the relation

$$g_1(\alpha^{(n-1)})=g_i\left(\frac{\pi}{2}+\alpha^{(n-1)}\right)=g_{-1}(\pi+\alpha^{(n-1)})$$

$$=g_{-i}\left(\alpha^{(n-1)}-\frac{\pi}{2}\right), \quad (28)$$

for the distribution shown in Fig. 3(a). Thence, we determine the density $g_1(\alpha^{(n-1)})$, and the densities of other $(n-1)$ cycles are followed from $g_1(\alpha^{(n-1)})$ according to the above relation.

Because that the inverse map given by Eq. (16) is 1 to 4 and the $(n-1)$ cycle of $z_0=1$ is a descendant of the left n cycle, we can express the density $g_1(\alpha^{(n-1)})$ as

$$g_1(\alpha^{(n-1)})=\frac{g_+(\alpha^{(n)})}{4}\left|\frac{d\alpha^{(n)}}{d\alpha^{(n-1)}}\right|. \quad (29)$$

To determine the transformation Jacobian $|d\alpha^{(n)}/d\alpha^{(n-1)}|$, we first notice that the $(n-1)$ cycles of $z_0=\pm1$ are the solutions of the equation

$$|\tanh(\eta^{(n-1)})|^4-\{[\tanh(\eta^{(n-1)})]^2+[\tanh\eta^{(n-1)*}]^2\}$$

$$-2\sqrt{2}|\tanh(\eta^{(n-1)})|^2+1=0, \quad (30)$$

where $\tanh(\eta^{(n-1)*})$ is the complex conjugate of $\tanh(\eta^{(n-1)})$. This result is obtained by substituting Eq. (15) into Eq. (14) for the left n cycle. By further substituting Eq. (27) with $z_0=1$ into Eq. (30), we obtain

$$r^4+r^3[4\cos(\alpha^{(n-1)})]+r^2(4-2\sqrt{2})$$

$$-r[4\sqrt{2}\cos(\alpha^{(n-1)})]-2\sqrt{2}=0. \quad (31)$$

This equation can be solved numerically to obtain $r(\alpha^{(n-1)})$ and $dr/d\alpha^{(n-1)}$. Moreover, the relation between $\alpha^{(n)}$ and $\alpha^{(n-1)}$ has been specified by the map of Eq. (15). We substitute Eqs. (21) and (27) into Eq. (15) to obtain

$$1+\sqrt{2}\exp(i\alpha^{(n)})=\frac{2[1+r(\alpha^{(n-1)})\exp(i\alpha^{(n-1)})]^2}{1+[1+r(\alpha^{(n-1)})\exp(i\alpha^{(n-1)})]^4}. \quad (32)$$

By differentiating this equation with respect to $\alpha^{(n-1)}$ and by using the known values of $r(\alpha^{(n-1)})$ and $dr/d\alpha^{(n-1)}$, we can determine the derivative $d\alpha^{(n)}/d\alpha^{(n-1)}$ and then obtain the density $g_1(\alpha^{(n-1)})$ according to Eq. (29).

The numerical result of the density $g_1(\alpha^{(n-1)})$ is shown in Fig. 3(b) for the range $0\leq\alpha^{(n-1)}\leq\pi$ with the radial distance of a zero, $r(\alpha^{(n-1)})$, specified in the right vertical scale. Our results indicate that when the complex plane changes from $\tanh(\eta^{(n)})$ to $\tanh(\eta^{(n-1)})$, the distribution density oscillates more rapidly with the peak number increasing from 2 to 4 for half cycle. The locus of the zero corresponding to the ferromagnetic phase transition point moves from $\alpha^{(n)}=0$ of the left n cycle to $\alpha^{(n-1)}=\pi$ of the $(n-1)$ cycle of $z_0=1$. For the zeros near to $\alpha^{(n-1)}=\pi$, the density has the linear behavior as

$$g_1(\pi+\alpha^{(n-1)})=\delta_1\left(\frac{3+2\sqrt{2}}{\pi}\right)|\alpha^{(n-1)}|, \quad (33)$$

with

$$\delta_1=\frac{1}{4}\left|\frac{d\alpha^{(n)}}{d\alpha^{(n-1)}}\right|_{\alpha^{(n-1)}=\pi}=0.1529. \quad (34)$$

This linear behavior, again, gives the logarithmic singularity of the specific heat.

To extend the calculation of density to $(n-2)$ cycles, we may divide the 12 $(n-2)$ cycles shown in Fig. 4(a) into three classes named as class I, II, and III, according to the decreasing order from the longest to the smallest in the magnitude of the circumference of the circles. Then, there are four members in each class, and all members of class I are the descendants of the left n cycle and those belonging to classes II and III are from the right n cycle. Similar to the case of $(n-1)$ cycles, we can write

$$\tanh(\eta^{(n-2)})=z_1+r(\alpha^{(n-2)})\exp(i\alpha^{(n-2)}) \quad (35)$$

for the zeros of $(n-2)$ cycles, and the center coordinates z_1 are chosen to be the preimages of the map of Eq. (15) for the center coordinates of $(n-2)$ cycles, 1, -1, i, and $-i$. Then, we can express the densities of the $(n-2)$ cycles as

$$g_{z_1}^I(\alpha^{(n-2)}) = \frac{g_1(\alpha^{(n-1)})}{4} \left| \frac{d\alpha^{(n-1)}}{d\alpha^{(n-2)}} \right|, \qquad (36)$$

and

$$g_{z_1}^{II,III}(\alpha^{(n-2)}) = \frac{g_i(\alpha^{(n-1)})}{4} \left| \frac{d\alpha^{(n-1)}}{d\alpha^{(n-2)}} \right|, \qquad (37)$$

respectively, where the superscript I, II, or III is used to denote the class to which a $(n-2)$ cycle belongs, and the subscript, z_1, is used to specify a $(n-2)$ cycle in the given class. Since the members belonging to the same class are the same up to a global rotation, we only need to determine the zero density of a $(n-2)$ cycle for each class. The cycles of $z_1 = 1$, $\sqrt{1+\sqrt{2}} e^{i\pi/4}$, and $\sqrt{-1+\sqrt{2}} e^{i\pi/4}$, belonging to classes I, II, and III, respectively, are choosen for the calculation of the density of the respective class.

The numerical method of calculating the correspondence between $\alpha^{(n-1)}$ and $\alpha^{(n-2)}$ and the Jacobians $|d\alpha^{(n-1)}/d\alpha^{(n-2)}|$ are exactly the same as we did in the last case. The results of $r(\alpha^{(n-2)})$ (right vertical scale) and $g(\alpha^{(n-2)})$ (left vertical scale) are shown in Figs. 4(b), 4(c), and 4(d), respectively, for the three cycles. These results indicate that the rapidity of oscillation in the distribution density of the cycles of class I increases as the peak number doubles with respect to the last case, while the peak number remains to be the same for the cycles of classes II and III. The zero corresponding to the critical point of ferromagnetic phase transition moves from $\alpha^{(n-1)} = \pi$ of the $(n-1)$ cycle of $z_0 = 1$ to $\alpha^{(n-2)} = \pi$ of the $(n-2)$ cycle of $z_1 = 1$ of class I. The density of the zeros near to this locus has the linear behavior

$$g_{z_1=1}^I(\pi + \alpha^{(n-2)}) = \delta_2 \left(\frac{3+2\sqrt{2}}{\pi} \right) |\alpha^{(n-2)}|, \qquad (38)$$

with

$$\delta_2 = \left(\frac{1}{4} \right)^2 \left(\left| \frac{d\alpha^{(n-1)}}{d\alpha^{(n-2)}} \right|_{\alpha^{(n-2)}=\pi} \right) \left(\left| \frac{d\alpha^{(n)}}{d\alpha^{(n-1)}} \right|_{\alpha^{(n-1)}=\pi} \right)$$

$$= 0.0365. \qquad (39)$$

From the densities obtained in the above, we may conjecture qualitatively the density of the 0 cycles with $n=4$ shown in Fig. 5 as the following: There are 128 members belonging to the descendants of the $(n-2)$ cycles of classes II and III, as displayed by bold-faced curves in Fig. 5. The 16 members of the 128, appearing in the outermost of Fig. 5,
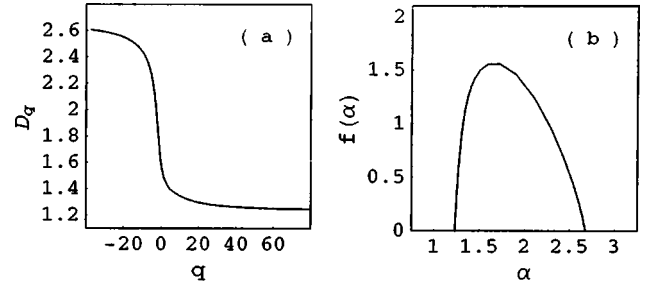

FIG. 7. (a) The generalized dimension D_q and (b) the singularity spectrum $f(\alpha)$ of the Julia set associated with the renormalization map.

are similar to a $(n-2)$ cycle of class II, and the rest have a similar shape as a $(n-2)$ cycle of class III. Up to an overall reduction factor, the densities of the 16 members have the same oscillation pattern as that shown in Fig. 4(c) and the densities for the rest members possess the same oscillation pattern that shown in Fig. 4(d). For the 44 descendants of the $(n-2)$ cycles of class I displayed by gray curves in Fig. 5, the corresponding density reduces but oscillates more rapidly with 32 peaks in half cycle in comparing with that shown in Fig. 4(b).

Continuing with this procedure in finding the density, we obtain 2^{n+1} peaks in a π period for each of the 0 cycles, which are the descendants of the left n cycle. On the other hand, the peak number always maintain to be 4 for each of the 0-cycles belonging to the descendants of the right n cycle along with the decreasing radius as n increases.

V. JULIA SET AND INFINITE N LIMIT

The recursion relation given by Eq. (15) happens to be a rational map of degree 4. Then, from the work of Julia and Fatou, we may conclude that the backward iterations defined by Eq. (16) leads towards the Julia set associated with the map of Eq. (15).

Generally, Julia sets can be divided into two classes: some are connected in one piece while the others are just a cloud of points. The tendency of the zero density with increasing n shown in the above section indicates that the Julia set here belongs to the latter. Moreover, by observing the distribution patterns and the densities of the zeros, we may conclude that a 0 cycle belonging to the descendants of the right n cycle shrinks to a point in the limit of infinite n, and these infinite number of points coincide not only with the 0 cycles generated from the left n cycle but also with the zeros obtained from the condition $\tanh(\eta^{(n-1)}) = \pm i$ for infinite n. Thus, the same Julia set arises in DHIM as well as DDIM in the infinite limit. In fact, the loci of the zeros of DDIM in the infinite limit are identical to that of DHIM.

The Julia set arising from the distribution of the Fisher zeros possesses multifractal structure, and the corresponding generalized dimensions D_q and singularity spectrum $f(\alpha)$, obtained by using derivative method and by approximating the limiting set of the zero distribution with that of $n=8$ shown in Fig. 6 [14,15], are shown in Fig. 7.
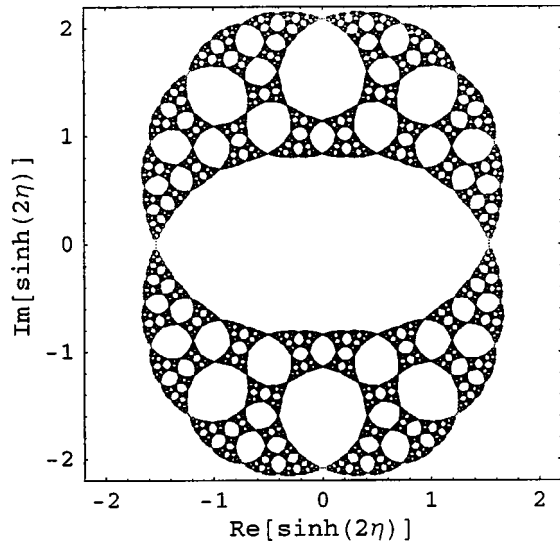
FIG. 8. The zero distribution of an n lattice in the complex $\sinh(2\eta)$ plane obtained from the condition of Eq. (12) for $n=8$.

The $\sinh(2\eta)$ complex plane is also widely used in studying the distribution of the zeros for simple square Ising model. The results of simple square Ising model imply that the zeros may lie on the unit circle $|\sinh 2\eta^{(n)}|=1$, for an n lattice. To obtain the distribution in the $\sinh(2\eta)$ complex plane, starting with the unit circle we then perform n fold backward iterations of the map,

$$\sinh(2\eta^{(n)}) = \frac{1}{2}\left[\frac{[\sinh(2\eta^{(n-1)})]^4}{1+[\sinh(2\eta^{(n-1)})]^2}\right.$$
$$\left. + \frac{2[\sinh(2\eta^{(n-1)})]^2}{1+[\sinh(2\eta^{(n-1)})]^2}\right], \qquad (40)$$

which is an equivalent expression of Eq. (6). This is also a rational map of degree 4, and the Julia set associated with this map can be approximated with n fold backward iterations for a sufficiently large n. The resultant distribution of $n=8$ are shown in Fig. 8. Though the distribution pattern is different from that in the complex $\tanh(\eta)$ plane shown in Fig. 6, owing to the fact that Julia set is an invariant set, the global multifractal structure characterized by D_q and $f(\alpha)$ is the same as that shown in Fig. 7.

The density near the bulk transition point has a linear behavior, and the linear behavior gives the logarithmic singularity of the specific heat. By observing the results of Eqs. (26), (33), and (38), we may expect that the linear behavior for the density near the bulk transition point disappears in the limit of infinite n. This leads to the nondiverging behavior in the specific heat as the decoration level goes infinite [24].

VI. SUMMARY AND DISCUSSION

In summary, we study the distribution and the density of the Fisher zeros for the Ising model defined on square lattices with diamond-type bond decorations in this paper. By carrying out the exact renormalization map of temperature, we can express the free energy of an n lattice as the sum of two parts: one, referred as the local part, is mainly the contribution from an n level decorated bond and the other, referred as the long-range part, is the contribution from the interactions among n level decorated bonds. For the local part, we obtain the zeros as a set of scattered points. Along with the increase in the number of the scattered points in the distribution of the zeros as the decoration level n increases, all zeros belonging to the lower decoration levels are also contained in the distribution of zeros of the higher decoration level. The corresponding zeros of the long-range part are the union of continuous closed curves, which also form subrings due to the intersections. For the long-range part, the distribution of the zeros leads towards the Julia set associated with the renormalization map, which is a rational map of degree 4. This Julia set also serves as the limiting set of the zeros obtained from the local part of the free energy. The zero representing the critical point of ferromagnetic phase transition is one of the zeros of the long-range part in the physical region, and the locus of the critical point for an arbitrary decoration level n is given. Along with the distribution pattern, we also calculate the density of the zeros of the long-range part for the cases of $n=1$ and 2. The evolution of the density of zeros in the course of increasing n indicates that the Julia set is a cloud of points. Thus, the Julia set has the Hausdorff dimension greater than 1 and possesses the multifractal structure.

Comparing with the continuous closed curves appearing in the distribution of zeros of the simple square Ising model, we have more complicated distribution patterns for the bond-decorated Ising model. The patterns remain to be continuous closed curves in both $\tanh(\eta)$ and $\sinh(2\eta)$ complex planes for a finite decoration level n, and only in the limit of infinite n the continuous closed curves break into areas that contain multifractal structure. It has been demonstrated on classic lattices that when the couplings among the nearest neighbors change from isotropic to anisotropic, the distribution of the Fisher zeros may change from continuous curves to an area in the plane [19,20]. However, the converse is not necessary to be true as the example shown in Ref. [26]. In regard to the bond-decorated Ising model, the interactions among the Ising spins are effectively isotropic after the renormalization map to the corresponding 0 lattice, although the coordination numbers of lattice sites are highly inhomogeneous for an n lattice with large n. This leads to the conclusion that in the limit of infinite decoration levels the system has completely different properties: The distribution of the zeros has multifractal structures, and the nature of phase transition of the system is different from that of finite decoration levels [24].

[1] R.B. Griffiths and M. Kaufman, Phys. Rev. B **26**, 5022 (1982).

[2] N.M. Svrakic, J. Kertesz, and W. Selke, J. Phys. A **15**, L427 (1982).

[3] B. Derrida, J.P. Eckmann, and A. Erzan, J. Phys. A **16**, 893 (1983).

[4] M. Kaufman and R.B. Griffiths, Phys. Rev. B **24**, 496 (1981).

[5] A. Erzan, Phys. Lett. **93A**, 237 (1983).

[6] B. Derrida, L.De. Seze, and C. Itzykson, J. Stat. Phys. **33**, 559 (1983).

[7] B. Derrida, C. Itzykson, and J.M. Luck, Commun. Math. Phys. **94**, 115 (1985).

[8] F.T. Lee and M.C. Huang, J. Stat. Phys. **75**, 1119 (1994).

[9] F.T. Lee and M.C. Huang, Chin. J. Phys. (Taipei) **37**, 398 (1999).

[10] A.A. Migdal, Sov. Phys. JETP **42**, 743 (1976).

[11] L.P. Kadanoff, Ann. Phys. (N.Y.) **100**, 359 (1976).

[12] A.N. Berker and S. Qstlund, J. Phys. C **12**, 4961 (1979).

[13] M.H. Jensen, L.P. Kadanoff, and I. Procaccia, Phys. Rev. A **36**, 1409 (1987).

[14] B. Hu and B. Lin, Phys. Rev. A **39**, 4789 (1989).

[15] B. Hu and B. Lin, Physica A **177**, 38 (1991).

[16] C.Y. Yang and T.D. Lee, Phys. Rev. **87**, 404 (1952).

[17] T.D. Lee and C.Y. Yang, Phys. Rev. **87**, 410 (1952).

[18] M. E. Fisher, *Lecture Note in Theoretical Physics*, edited by W. E. Brittin (University of Colorado Press, Boulder, 1965), Vol. 7c, pp. 1–159.

[19] W. van Saarloos and D.A Kurtze, J. Phys. A **17**, 1301 (1984).

[20] J. Stephenson and R. Couzens, Physica A **129**, 201 (1984).

[21] H. Feldmann, R. Shrock, and S.H. Tsai, Phys. Rev. E **57**, 1335 (1998).

[22] C.N. Chen, C.K. Hu, and F.Y. Wu, Phys. Rev. Lett. **76**, 169 (1996).

[23] W.T. Lu and F.Y. Wu, J. Stat. Phys. **102**, 953 (2001).

[24] M.C. Huang, Y.P. Luo, and T.M. Liaw, Physica A **321**, 498 (2003).

[25] T.M. Liaw, M.C. Huang, Y.L. Chou, and S.C. Lin, Phys. Rev. E **65**, 066124 (2002).

[26] W. Janke, D. Johnston, and R. Kenna, e-print hep-lat/0208014.